Supporting Information

for

cis-Tetrachlorido-bis(indazole)osmium(IV) and its osmium(III) analogues: paving the way towards the *cis*-isomer of the ruthenium anticancer drugs KP1019 and/or NKP1339

Gabriel E. Büchel,[#,§] Susanne Kossatz,[§] Ahmad Sadique,[§] Peter Rapta,*[,▽] Michal Zalibera,[▽] Lukas Bucinsky,[▽] Stanislav Komorovsky,[◊] Joshua Telser,*[,⊥] Jörg Eppinger,[#] Thomas Reiner,[§,Δ] Vladimir B. Arion*[,‖]

[#]Division of Physical Sciences and Engineering, KAUST Catalysis Center, King Abdullah University of Science and Technology, Thuwal 23955-6900, Saudi Arabia

[§]Department of Radiology, Memorial Sloan Kettering Cancer Center, 1275 York Avenue, New York, New York, USA

[▽]Slovak University of Technology, Institute of Physical Chemistry and Chemical Physics, Radlinského 9, 81237 Bratislava, Slovakia

[◊]Institute of Inorganic Chemistry, Slovak Academy of Sciences, Dúbravská cesta 9, SK-84536, Slovakia

[⊥]Department of Biological, Chemical and Physical Sciences, Roosevelt University, 430 S Michigan Avenue, Chicago, Illinois 60605, USA

[Δ]Department of Radiology, Weill Cornell Medical College, New York, NY 10065, USA

[‖]University of Vienna, Faculty of Chemistry, Institute of Inorganic Chemistry, Währinger Str. 42, A-1090 Vienna, Austria

Osmium(IV), osmium(III), 1*H*-indazole, cis/trans isomerism, solvatochromism, antiproliferative activity, EPR spectra

RECEIVED DATE (to be automatically inserted after your manuscript is accepted)

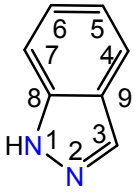

Figure S1. Atom numbering scheme for NMR resonances assignment.

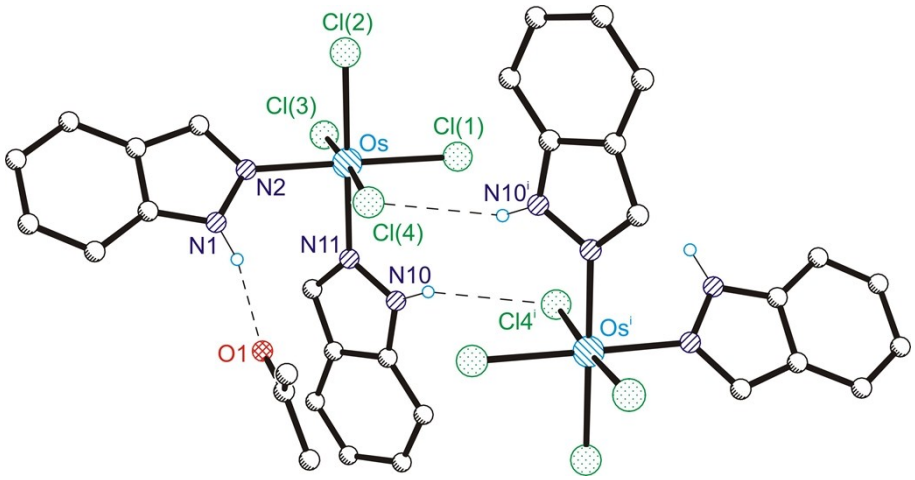

Figure S2. Part of the crystal structure of [**1**]·Me_2CO showing intermolecular hydrogen bonding interactions. Parameters of hydrogen bonding interactions N1–H···O1 [N1···O1 2.740(3) Å, N1–H···O1 163.1°], N10–H···Cl4^{i}(–*x* + 2, –y, –z + 1) [N10···Cl4^{i} 3.316(2) Å, N10–H···Cl4i 137.7°].

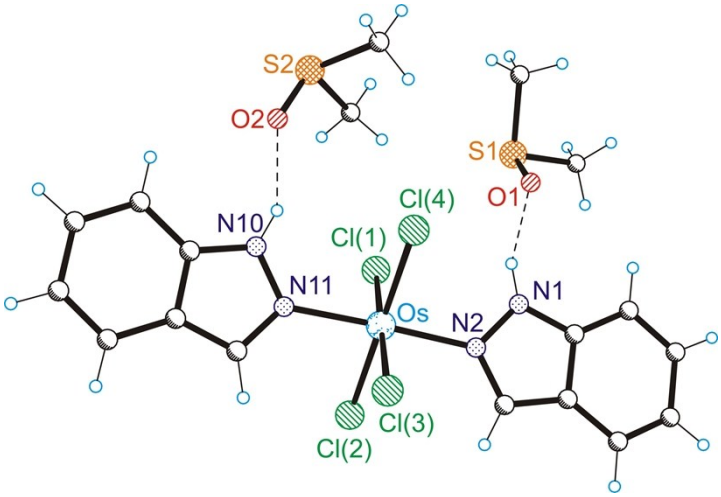

Figure S3. Part of the crystal structure of [**2**]·2DMSO showing intermolecular hydrogen bonding interactions. Parameters of hydrogen bonding interactions N1–H···O1 [N1···O1 2.705(4) Å, N1–H···O1 155.6°], N10–H···O2 [N10···O2 2.677(4) Å, N10–H···O2 148.1°].

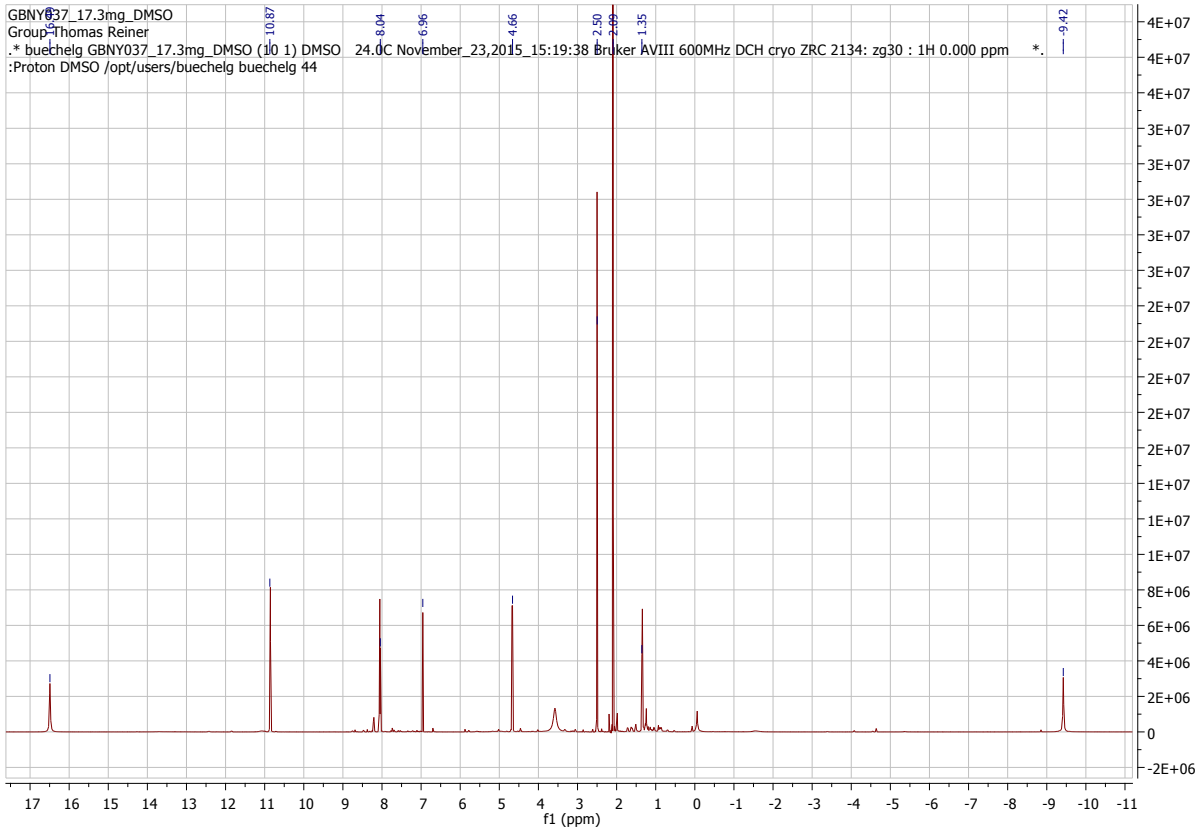

Figure S4. ^{1}H NMR spectrum of [**1**] in Me_2SO-d_6. The resonance at 6.96 ppm is due to 1,1,2,2-tetrachloroethane.

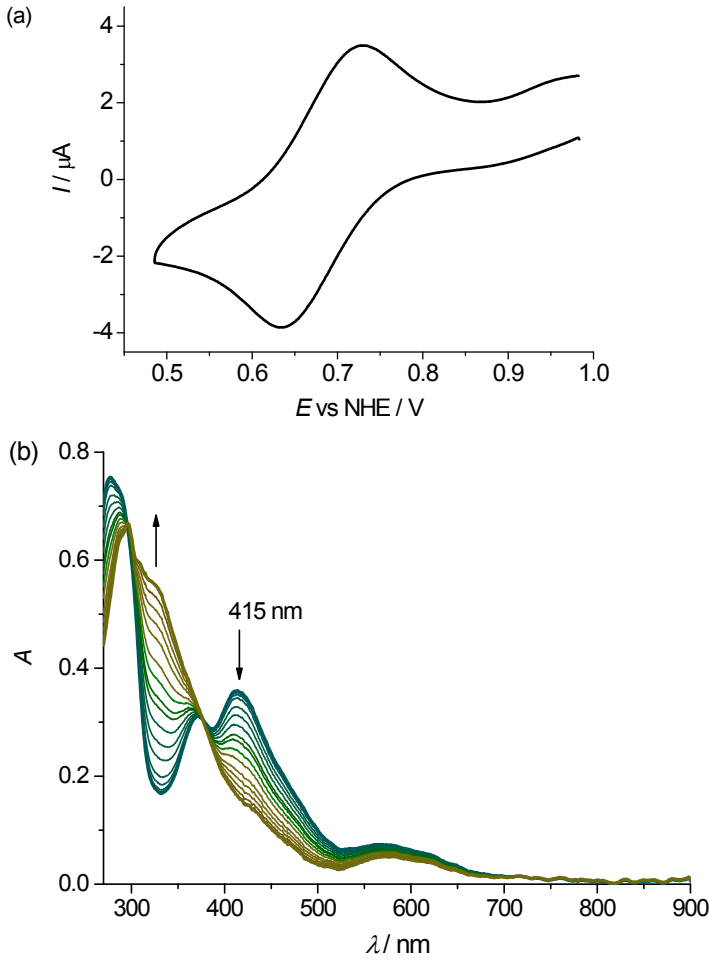

Figure S5. In situ UV-vis-NIR spectroelectrochemistry for [**1**] in 0.2 M nBuN$_4$[PF$_6$] in DMSO (scan rate 5 mV s^{-1}, Pt-microstructured honeycomb working electrode): (a) the corresponding *in situ* cyclic voltammogram; (b) UV-vis spectra detected simultaneously during the *in situ* reduction of [**1**] in the region of the first cathodic peak (from 1.0 V to 0.5 V vs NHE).

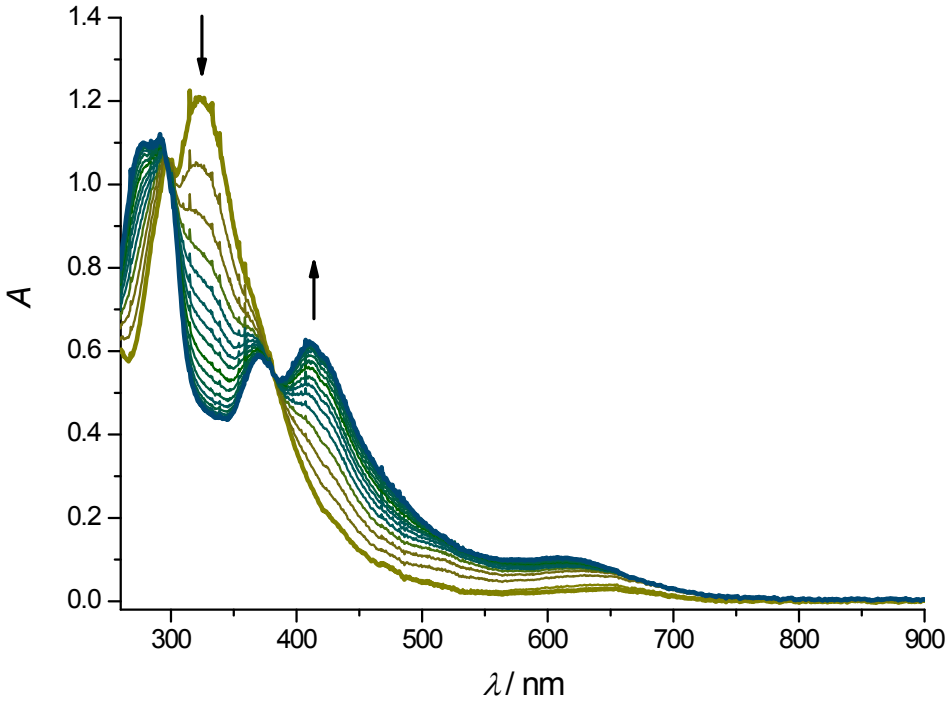

Figure S6. UV-vis spectra measured during electrochemical oxidation of (nBu$_4$N)[**1**] to [**1**] at 1.0 V vs NHE in 0.2 M nBuN$_4$[PF$_6$] in DMSO (thin layer cell with Pt-microstructured honeycomb working electrode, under argon).

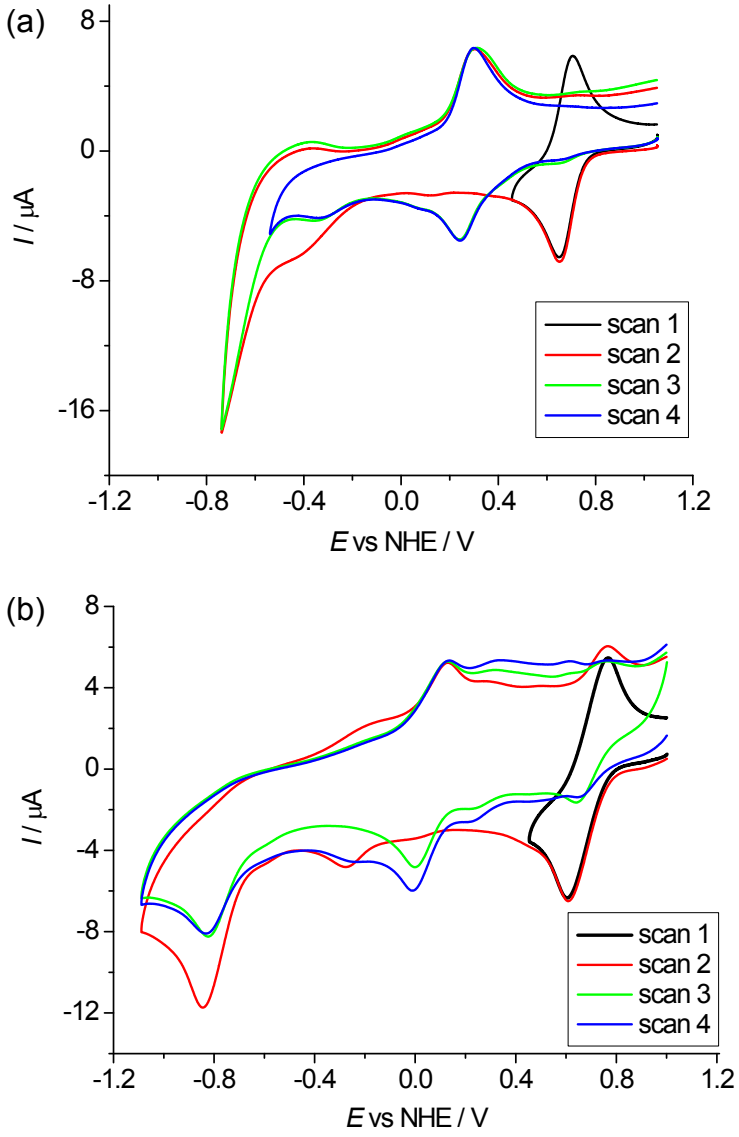

Figure S7. Cyclic voltammetry of [**1**] in 0.2 M nBuN$_4$[PF$_6$] in (a) acetonitrile and (b) in DMSO at scan rate of 10 mV s^{-1} using thin layer cell with the Pt-microstructured honeycomb working electrode (black trace – the first voltammetric scan in the region of the first reduction step, the second voltammetric scan going to the region of the second electron transfer, green and blue traces - the next two consecutive voltammetric scans going to the region of the second electron transfer.

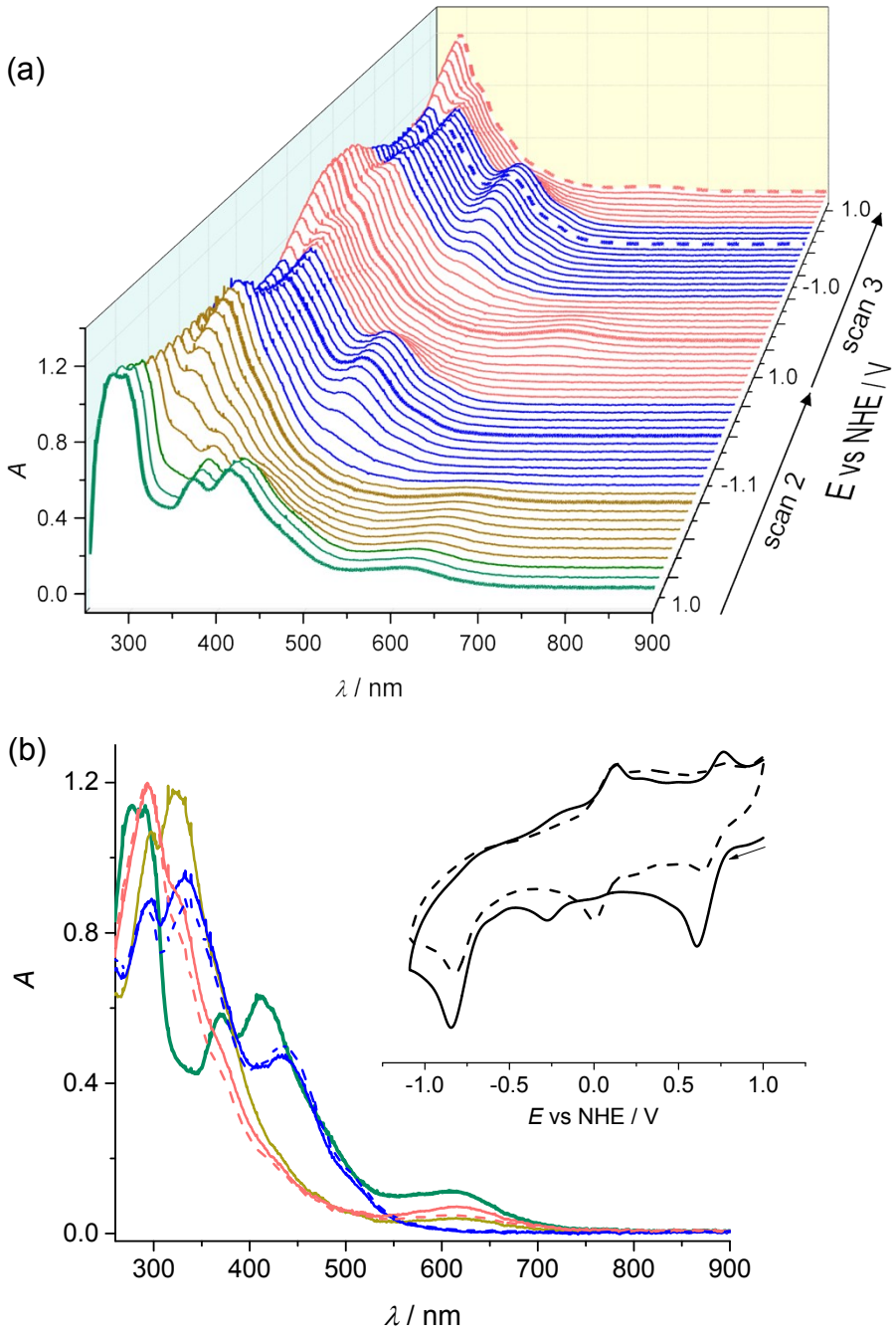

Figure S8. (a) UV-vis spectra monitored during the second voltammetric scan (see the corresponding CV in Figure S5 and solid trace in inset) of [**1**] in 0.2 M nBuN$_4$[PF$_6$]/DMSO solution going to the region of the second electron transfer as well as during the next consecutive voltammetric scan (see dashed trace in inset in a). (b) Selected UV-vis spectra taken at different potentials (see the corresponding thick selected lines in (a))

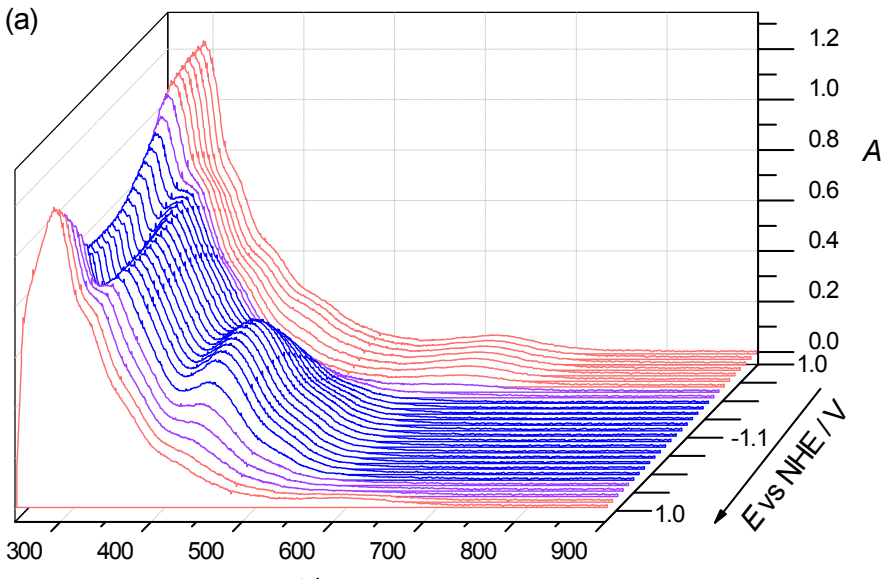

(b)

cis-[$Os^{IV}Cl_4$(κN2-1*H*-ind)$_2$]^0 $\underset{-e^-}{\overset{+e^-}{\rightleftharpoons}}$ cis-[$Os^{III}Cl_4$(κN2-1*H*-ind)$_2$]$^-$ $\underset{}{\overset{+e^-}{\rightleftharpoons}}$ cis-[$Os^{II}Cl_4$(κN2-1*H*-ind)$_2$]$^{2-}$

$\downarrow$ $-Cl^-$ $+Solv$

cis-[$Os^{III}Cl_3$Solv(κN2-1*H*-ind)$_2$]^0 $\underset{-e^-}{\overset{+e^-}{\rightleftharpoons}}$ cis-[$Os^{II}Cl_3$Solv(κN2-1*H*-ind)$_2$]$^-$

Figure S9. (a) UV-vis spectra monitored during the fourth consecutive voltammetric scan (see the corresponding blue trace in Figure S5b) of [**1**] in 0.2 M nBuN_4[PF_6]/DMSO solution going to the region of the second electron transfer. (b) The proposed reaction scheme for cathodically induced metal dechlorination upon osmium(III) to osmium(II) reduction.

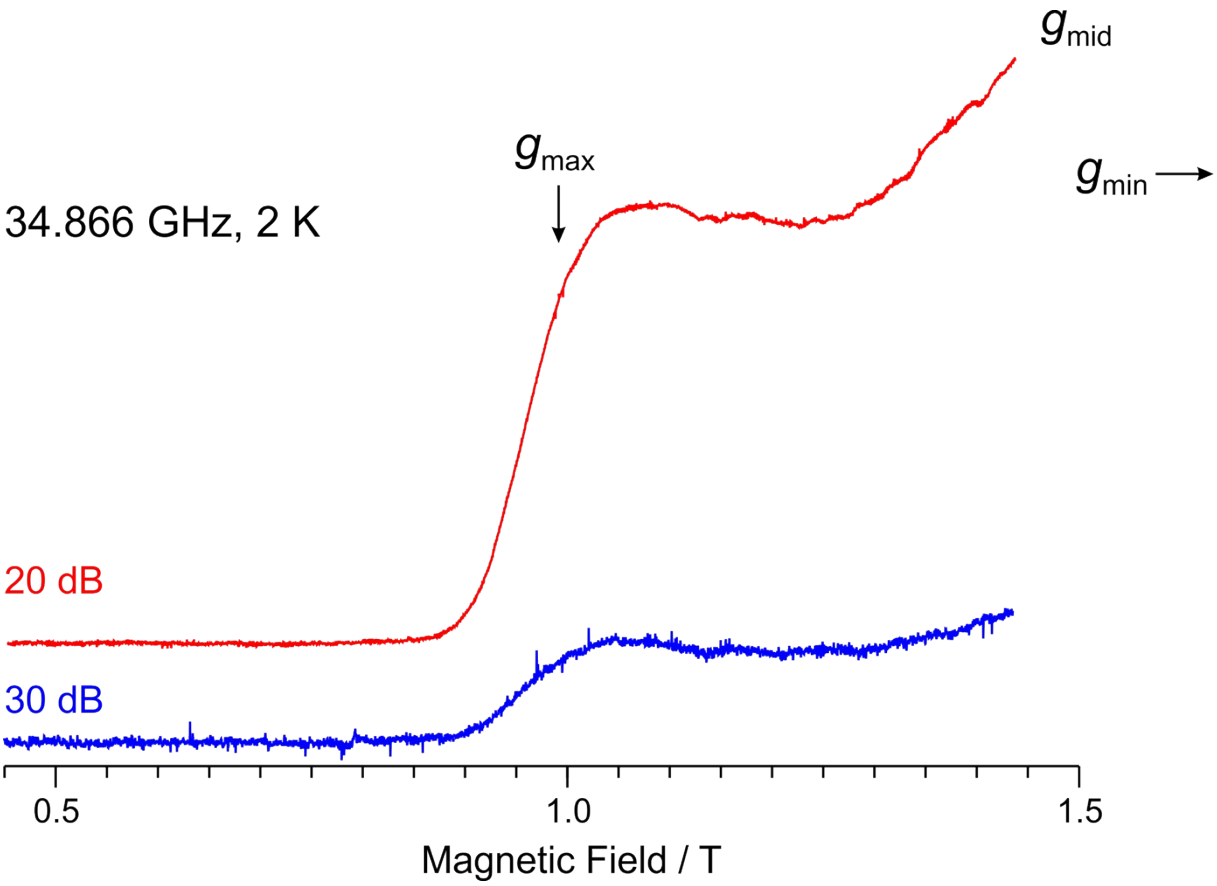

Figure S10. Q-band EPR spectrum of Na**[1]** in water/ethylene glycol 5:1 v/v recorded at 2 K. Under these conditions, the spin system is in "rapid passage" mode and appears as an absorption lineshape. Only the g_{max} feature is observable, and appears at $g_{obs} \approx 2.6$, in agreement with X-band measurements; the g_{mid} feature is just coming into field range, while the g_{min} feature is well beyond the maximum available magnetic field (~1.45 T; $g_{obs} \approx 1.72$). Two microwave powers are used, 20 dB (~2 mW; red trace) and 30 dB (~0.2 mW; blue trace). The substantial decrease in intensity at lower power (the receiver gain has been increased to compensate for this) indicates the fast electronic relaxation of this system.

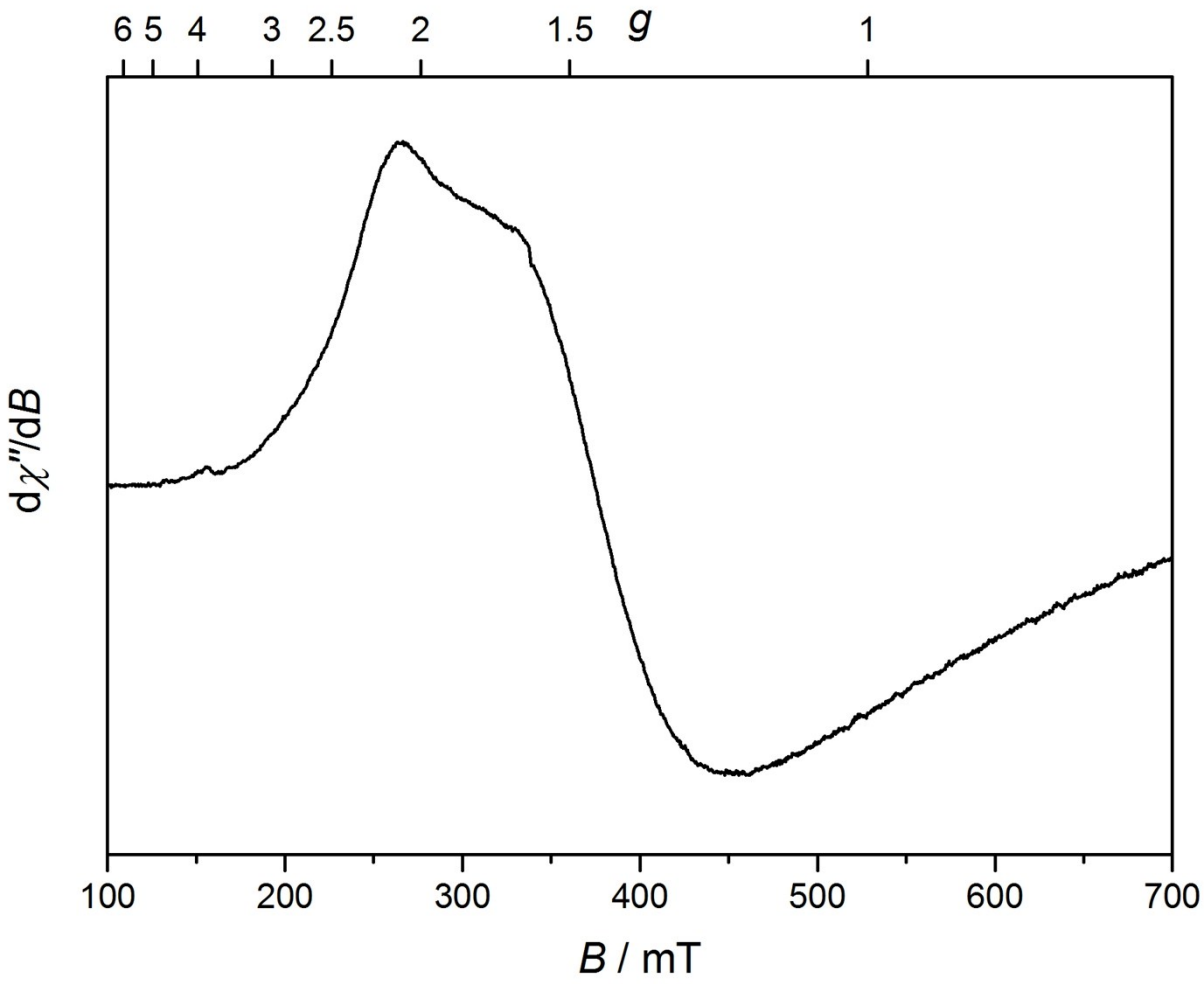

Figure S11. X-band EPR spectrum of nBu$_4$**[1]** powder sample recorded at 94 K.

Table S1. Results of Alamar Blue assay presented as IC_{50} (μM) values obtained after 48 h treatment.

	IC_{50} [μM]			
Complex	HT-29	H446	4T1	HEK293
[1]	75.7	56.7	126.6	72.6
Na[**1**]	179	20.5	75.0	118.8
[**3**]	70.4	49.4	>300	54.7
Cisplatin	58.6	7.7	28.7	43.2